

Plasma activation and bonding of crystalline thermoplastics

Dr. Stefan Nettesheim, Relyon Plasma GmbH, Weidener Str. 16, 93057 Regensburg, Germany
Stefan Reichlmaier, Physical Electronics GmbH, Fraunhoferstr. 4, 85737 Ismaning, Germany*

This article shows how the combination of chemical surface effects and remelting achieved by atmospheric plasma treatment produces an optimized structural bond for semi-crystalline thermoplastics. Polyoxymethylene (POM) is used as a model system.

Content

Introduction	1
Material and Adhesive System.....	2
Atmospheric Plasma System	2
Evaluation of the Surface Energy.....	2
Discussion	9
Summary	11

Introduction

Many thermoplastic materials are very difficult to bond. For polymers and composite materials, applying atmospheric pressure plasma for activation can be the most efficient method to improve adhesion. It is as well very cost-effective when used with compressed air. Plasma activation is compatible with virtually any serial process. Atmospheric plasma processes can in many cases replace chemical primers, which makes atmospheric plasma functionalization particularly environmentally friendly and gentle to materials. Fine cleaning, functionalization and compensation of the static surface charge are achieved in only one process step.

Even though plasma pretreatment can greatly enhance surface energy through functional groups directly at the surface, the resulting adhesive bonding is not always stronger. Especially with semi-crystalline polymers (such as e. g. POM or HD-PE), atmospheric plasma treatment with air significantly enhances the surface energy and, as a result, improves wettability considerably. However, this change in chemical surface characteristics does not necessarily improve the static friction force of the bond (e. g. with 2K epoxy glue or methyl methacrylate glue).

The glue adheres to the component surface through physical or chemical interactions. Especially for glues whose strength is developed through the polymerization of the monomers applied to the splice, there may occur diffusion and intercalation of monomers into the layer of glue close to the surface. Interlocking the polymer chains of the glue with polymer chains of the plastic substrate significantly enhances adhesion.

It is another practical observation that the adhesive force of glued plastic components decreases when stored in humid environments. Water absorption and the differing swelling behaviors of glue and substrate put stress on the interface, causing irreversible damage to the bonding.

Material and Adhesive System

Polyoxymethylene (POM; also called polyacetal, polyformaldehyde or acetal) was chosen as a model system. For our tests, we chose homopolymer (POM-H) for its degree of crystallization of up to 90%. Its intrinsic color is opaque white due to its high crystallinity and remains unchanged up to its melting temperature of ca. 175-178 °C (347-352 °F). At 220°C (428°F), POM starts to thermally disintegrate, releasing formaldehyde. Our sample was cut from extruded sheet products and blown dust-free clean with dry compressed air. For the adhesion tests, two common adhesive systems were used: a 2K epoxy resin system by Würth, and a modified 2K methacrylate system by ITW Plexus. The bonding was created maintaining constant gap dimensions and a defined bond area. Due to the measuring range of the extraction device with a limit of 500N, the bond area was limited to a diameter of 6mm for all tests, corresponding to an effective area of 28,3 mm². Using a shear test, the adhesive force was then read out of the force-path diagram and each test was repeated five times. Typically, variation between identically prepared samples was less than 10% and therefore entirely sufficient to make a valid statement on the shear breaking strength.

Atmospheric Plasma System

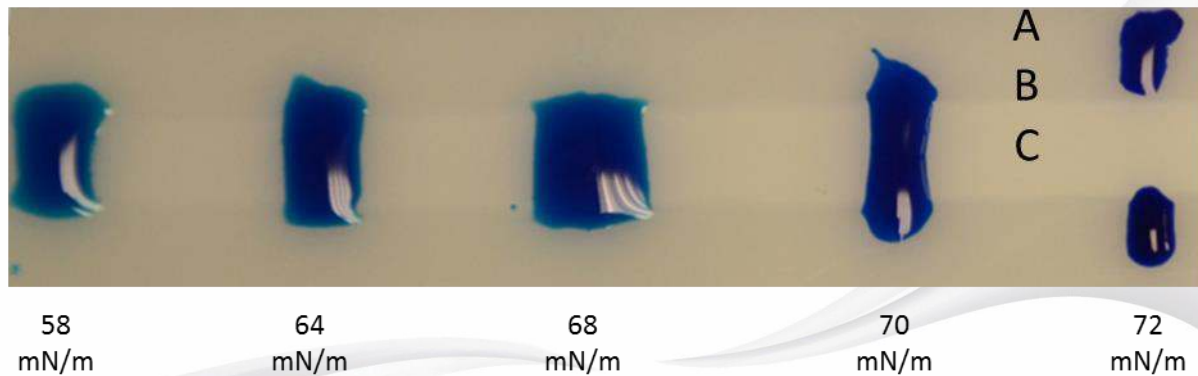
All tests were conducted using an integrated atmospheric plasma system (Plasmacell 300 by Relyon Plasma GmbH). All kinematic and geometric parameters and the power settings of the plasma flame can be adjusted in a reproducible way using the coordinating software. The device's movement dynamics allows for a relative velocity of up to 800mm/s, with high positioning accuracy.



Picture 1 Universally applicable plasma cell with xyz positioning unit (Plasmacell 300). Traversing speed of up to 800mm/s.

Evaluation of the Surface Energy

The wettability of the surface in question gives a first indication of the effectivity of the surface treatment. Wettability can easily be made visible by applying a liquid test ink. The ink test relies on the assumption that the solid body's free surface energy corresponds to the surface tension of the ink which only just manages to form a stable film on the sample. This method is quick to use, but rather imprecise as no distinction is made between the polar and the disperse proportion of the interaction. If various test inks with differing surface tensions are applied, the most important effects can be sufficiently illustrated. The respective wettable track gauges are especially well visible on a treated surface. The test inks used (according to the DIN ISO 8296 norm) were purchased from Ahlbrand.



Picture 2 Wettability behavior of the POM surface after plasma treatment (compressed air, $d=15\text{mm}$, $v=150\text{mm/s}$). It is obvious that the surface energy is highest directly at the edges of the visible track.

It is obvious how wettability is altered and surface energy is enhanced within a well-defined track. The qualitative statement based on simple test inks was supplemented by a contact angle measurement in order to break down the polar and disperse proportions of the surface energy. To this end, evaluations were carried out at different positions on the sample using the standard test liquids of water and diiodomethane according to Owens, Wendt, Rabel and Kaelble (OWRK). For each position, five measurements were performed and their results were averaged (Kaelble, 1970) (Owens & Wendt, 1969).

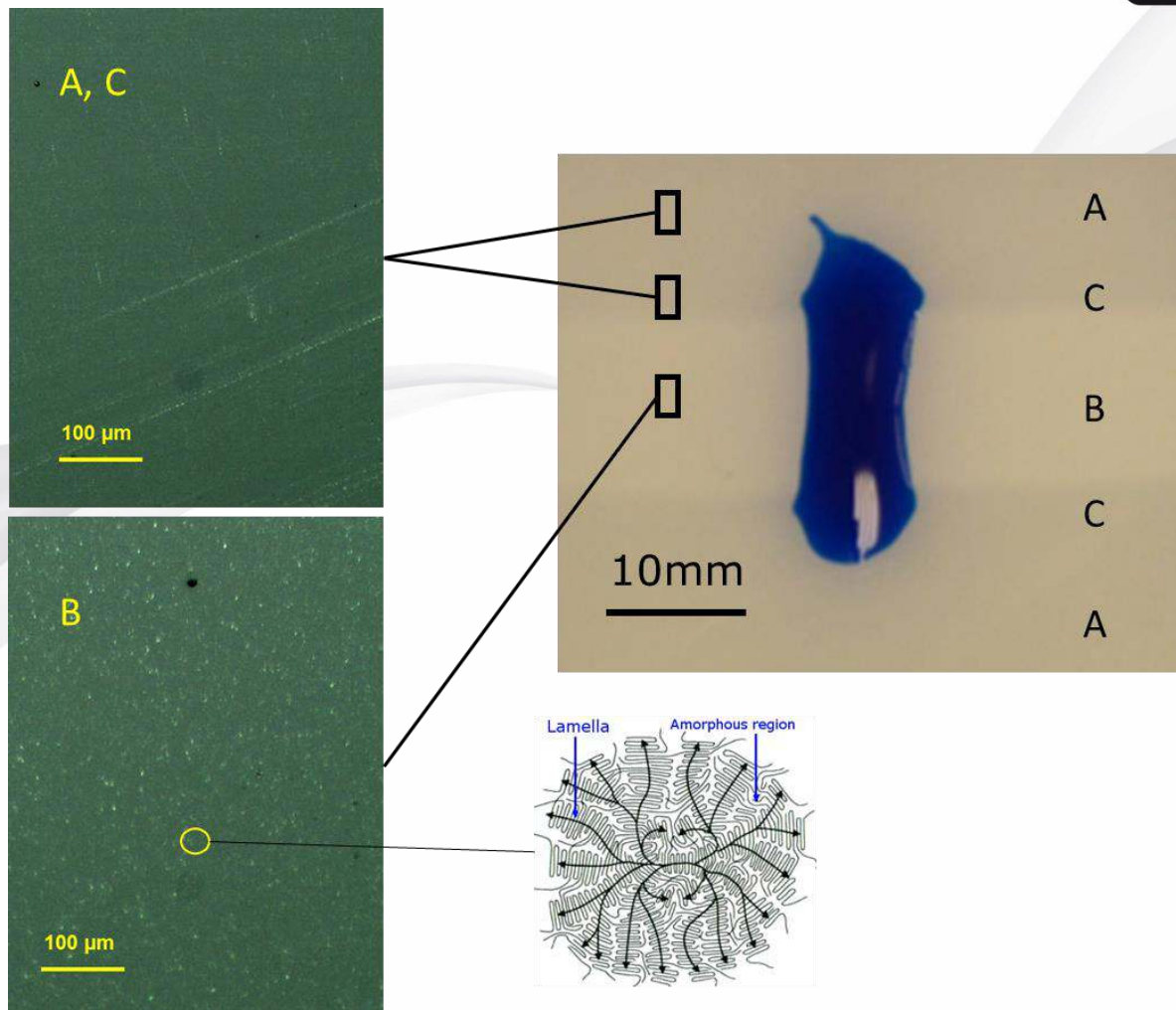
position of sample	disperse component of the free surface energy in mN/m	polar component of the free surface energy in mN/m	free surface energy in mN/m
A: untreated	35,7	6,9	42,6
B: track (middle)	35	9,4	44,4
C: track (edge)	38	9,6	47,6

Table 1 The qualitative effect observed in the ink tests also shows in the surface energy calculated from contact angle measurements. Altogether, it is striking that for POM, changes in surface energy are relatively minor.

It is striking that the increase in surface energy is altogether relatively minor and the highest surface energy is measured outside of the structurally altered track. Using nitrogen instead of compressed air as a plasma process gas changes the results only marginally.

Optical Microscopy

Even to the bare eye, the POM sample exhibits visible turbidity once a certain thermal stress is applied to the surface. However, and maybe contrary to expectation, this turbidity cannot be explained by any roughening of the surface within the μm scale. The fine granular structures rather point to the coexistence of semi-crystalline areas, embedded in an amorphized phase (Hemsley, 1989). If anything, slight irregularities such as scratches or point defects are evened out by plasma treatment. The optical appearance of a matt surface is due to the altered light refraction and the resulting diffuse dispersion.



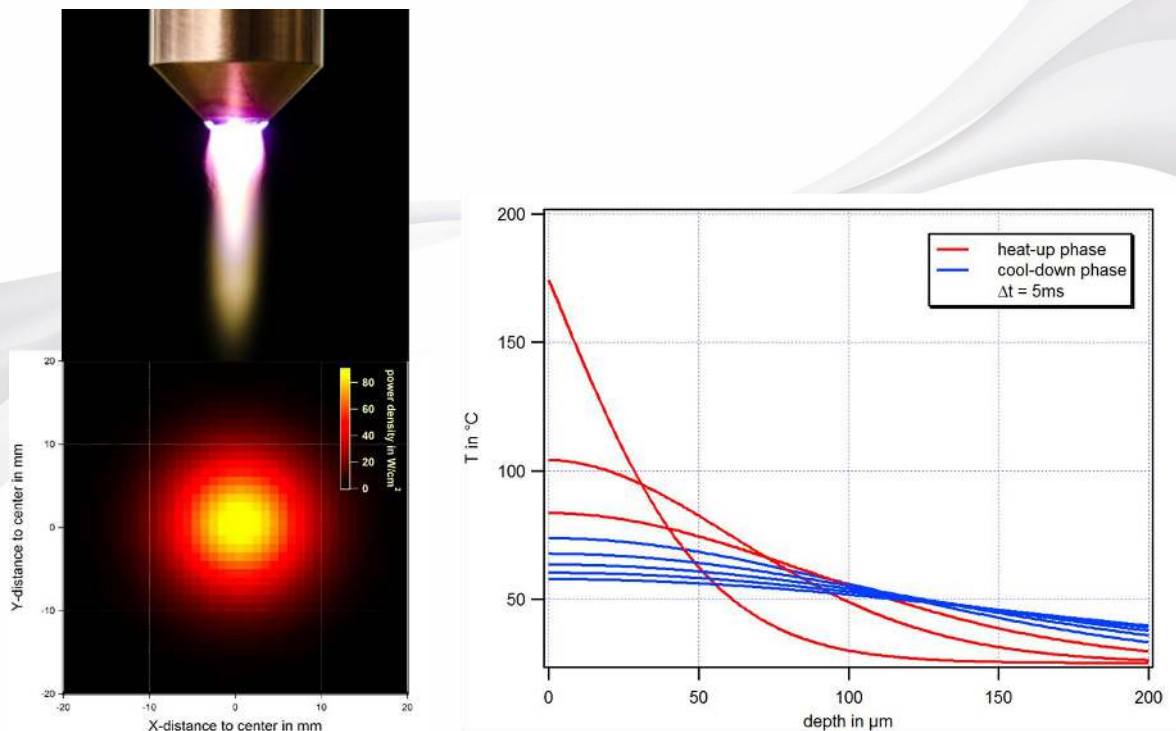
Picture 3 POM under the light microscope (incident light microscope type Nikon SMZ745T with camera adapter): untreated (A, C) and treated (B). Granular structures of ca. $5\mu\text{m}$ are visible. Fine surface artifacts such as slight scratches disappear on the area subjected to the plasma jet. It is a known fact that granular structures may occur when a polymer melt cools down rapidly and there is spherulite growth during the amorphous phase ([https://en.wikipedia.org/wiki/Spherulite_\(polymer_physics\)](https://en.wikipedia.org/wiki/Spherulite_(polymer_physics)))

Surface temperature

With the process parameters of the plasma flame kept constant, the surface temperatures and the depth distribution of temperature depend primarily on the working distance and the line speed as well as the thermal characteristics of the material treated.

Measurements of the surface temperature during the transit of the plasma flame were conducted using an infrared camera calibrated to the emission coefficient of the samples used, at 100 images/s. The possibility of disturbances of the camera system caused by the light emission of the plasma flame was tested and excluded. The systematic imprecisions of these measurements are largely due to the fact that only a very thin surface layer is effectively warmed up; additionally, the speed at which the material is heated and then cools down again is relatively high compared to the image frequency. The measurement data from the infrared camera are averaged over a depth of ca. $10\mu\text{m}$ and a time span of 10ms. This averaging leads to a systematic underestimation of the surface temperature. However, the temperature within the first 100nm of the surface is decisive for the kinetics of all surface-near processes, such as diffusion, desorption, and chemical functionalization, as well as phase transition processes and the restructuring of polymer chains.

The data of the power density effective on a surface as well as the spatial distribution are known for a given nozzle geometry and a defined working distance. When this known source of heat is applied to the sample, it is well possible to calculate the dynamic temperature distribution employing the heat equation and finite elements methods while using the known thermodynamic material constants.



Picture 4 The left picture shows the 20mm long plasma flame and coordinating power density which occurs at a distance of 15mm to the surface. The right picture shows the temporal development of the thermal depth profile in time increments of 5ms.

For the calculation, the measured power density distribution of the plasma generator in use is applied, and the device is moved across the substrate surface at the chosen speed.

The high dynamic with which the surface is heated and then cools down again rapidly is of particular interest in this case. If for example the traversal speed is 100mm/s, the heat/cool down rate may be over 5000K/s.

The following table compares the temperatures measured with the infrared camera to the surface temperatures resulting from calculation. As the infrared camera averages the temperatures with an integration time of 10ms and collects the infrared radiation from a depth of more than 10 µm, the temperatures for dynamic surface heating depicted by the IR camera are systematically too low.

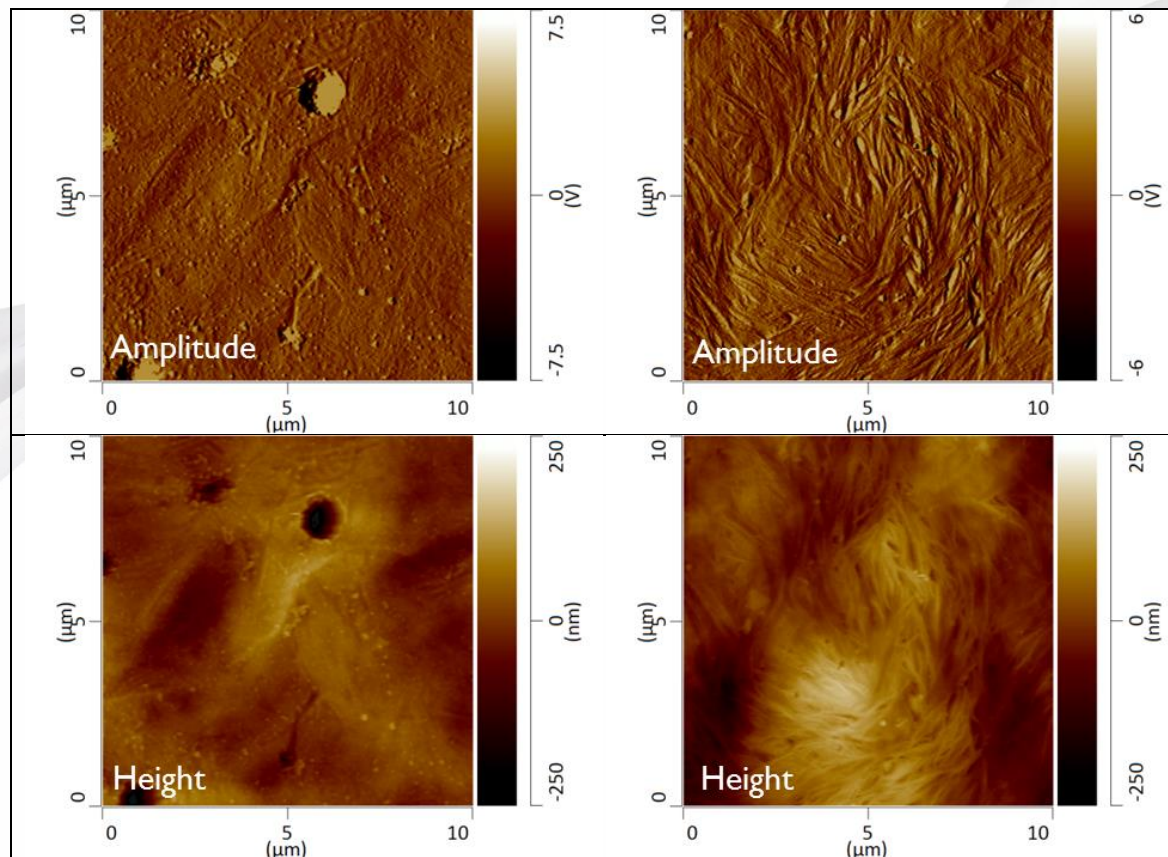
traversal speed [mm/s]	T _{IR} [°C]	T _{model} [°C]
200	115	155
150	124	175
100	150	209
50	219	(286)

Table 2 It is evident that the temperatures measured by the infrared camera are systematically lower than the calculated surface temperature (boundary layer to the plasma flame).

The calculated temperatures correspond reliably to the temperature threshold at which first turbidities become visible on the surface of POM..

Atomic Force Microscopy (AFM)

The surface topography can be viewed in high resolution by using atomic force microscopy (AFM) (Binnig, Quate, & Gerber, 1986). The resolution achieved may reach the atomic scale. Depending on mode of operation, information may be collected either on power or on topography.

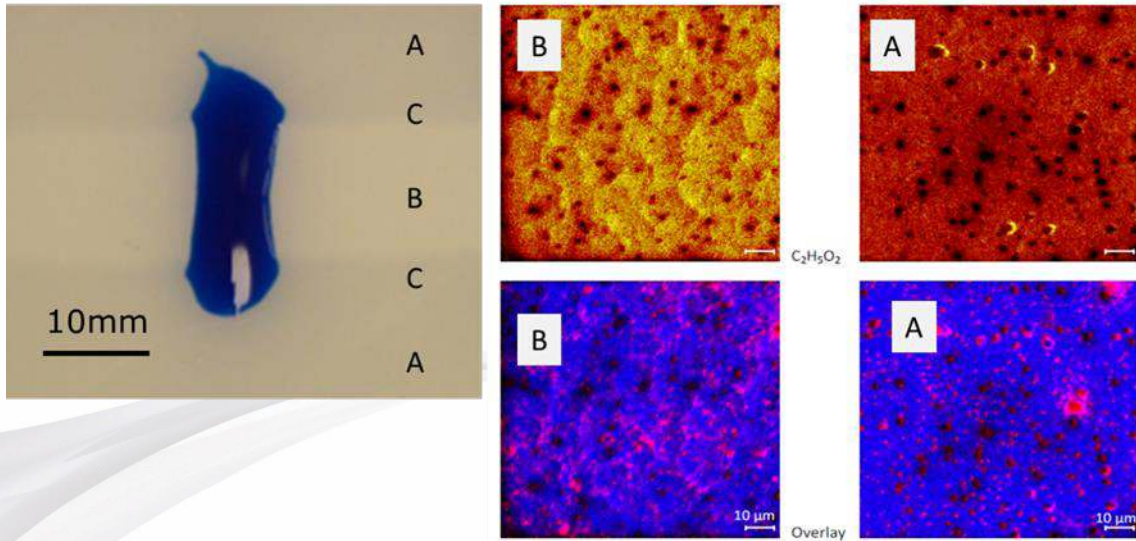


Picture 5 Amplitude and altitude information gained by AFM, which is operated in the so-called "non-contact-mode" in which the grid tip is moved very closely to the surface in an oscillating mode.

Mass Spectrometry (TOF-SIMS)

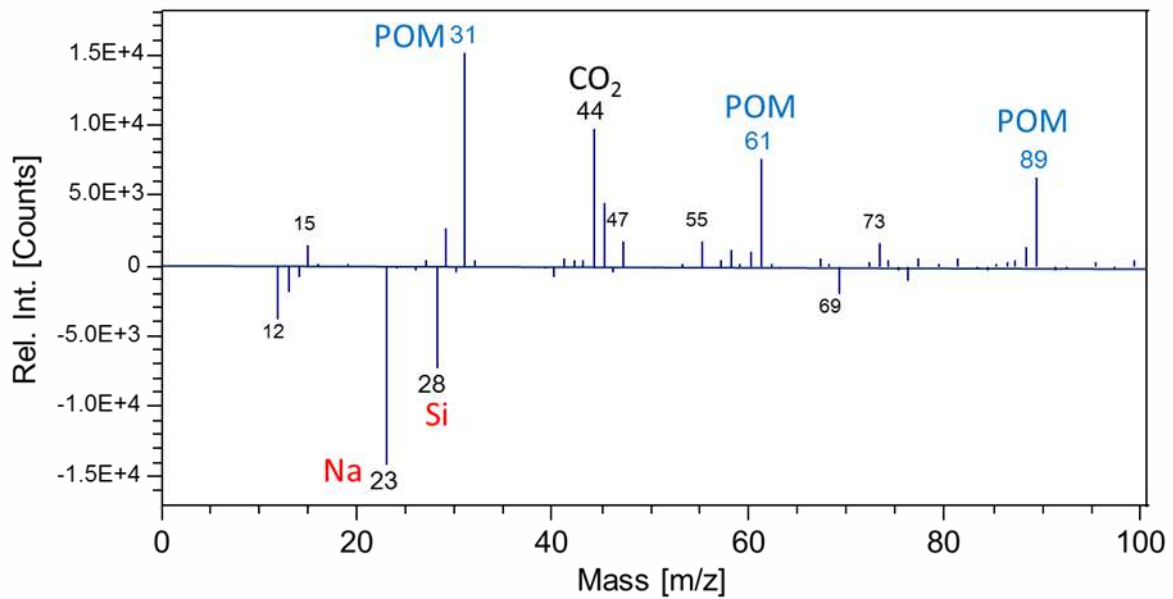
In order to conduct a chemical analysis of the surface which is both highly sensitive and provides detailed local resolution, the method which lends itself best is time of flight secondary ion mass spectrometry (TOF-SIMS). This method uses a pulsed primary ion beam in order to desorb secondary particles from the sample surface and ionize them (R. Seliger, 1979). These secondary ions are separated according to their mass by a mass spectrometer which measures their time of flight from the sample to the detector. The mass specters of secondary ions contain information about the surface's chemical composition. By scanning the sample surface with a focused ion beam, distribution images are recorded in order to display the distribution of different types of species across the surface ("imaging"). Due to the parallel mode of detection in TOF-SIMS, a complete mass specter is recorded in each pixel of the image. By sputtering the sample, depth profiles of the chemical elements are determined. This way, the composition and structure of a thin film can be specified.

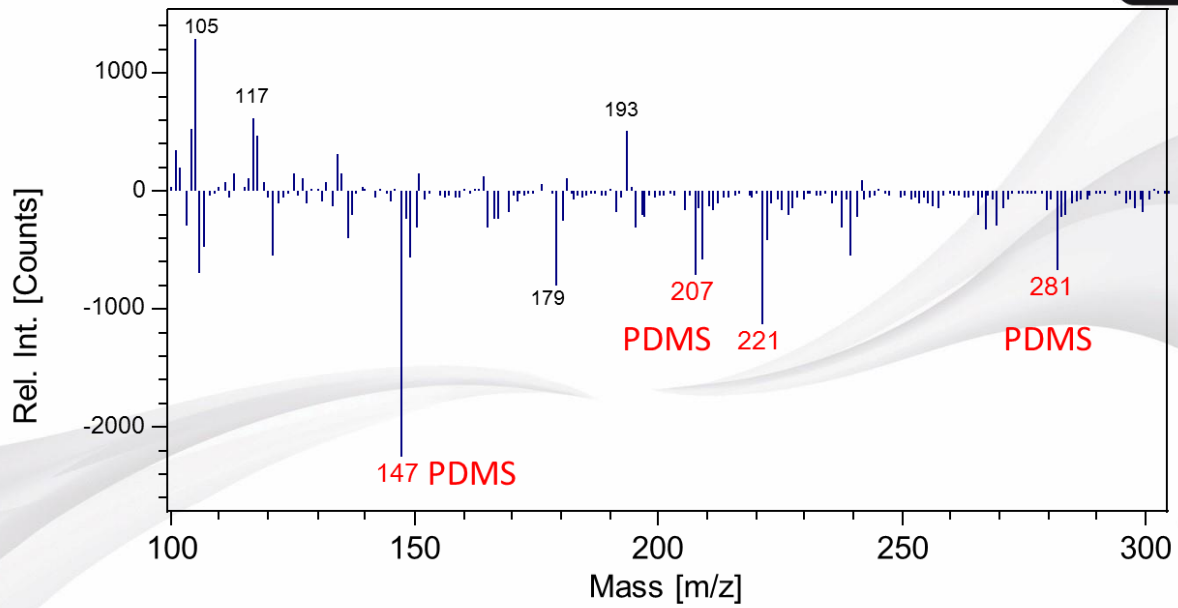
When TOF-SIMS is used on POM, what is mainly detected in the mass specter are the peaks typical of this material. The difference spectrum shows, however, that more sodium and silicon can be found on the untreated side of the sample. It also turn out that traces of a silicon-based polymer (polydimethylsiloxane, PDMS) can be detected in the untreated area, which is obviously (at least) reduced by plasma treatment.



Picture 6 Total intensity for POM characteristic line 8m061) and overlay (red=Na, blue=POM) before (A) and after (B) plasma exposition..

The fragmentary ion $C_2H_5O_2$ (mass 61) is characteristic of POM. Its distribution on the sample surface shows a clear difference between the treated and the untreated areas. The color overlays (red=Na, blue=POM) clearly demonstrate that the insular sodium distribution loses intensity and definition when treated. Obviously, sodium, which is a common contamination, is removed in the plasma process.



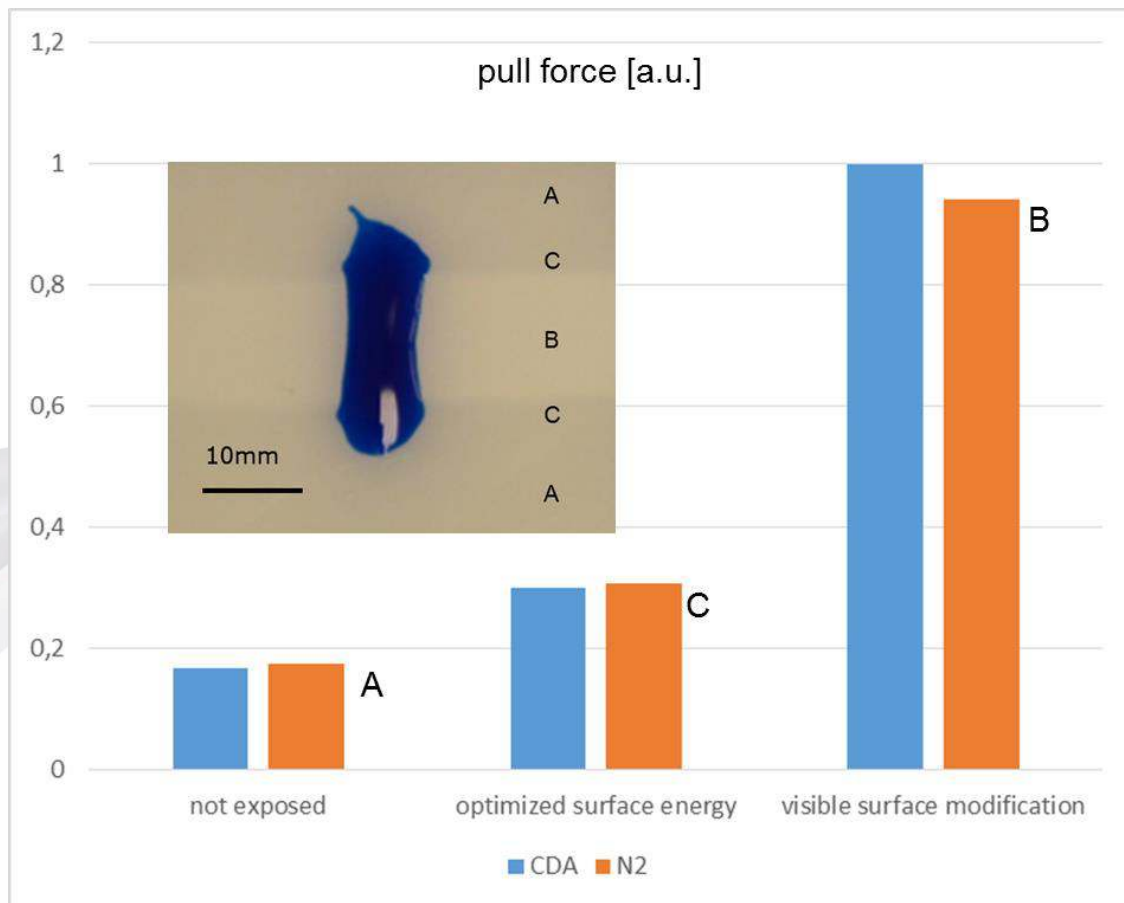


Picture 7 Normalized difference spectra (B-A) in the mass range between 0-100 and 100-300 Dalton.

Difference specters: First, the specters are standardized to total counts, then they are subtracted from each other. In the mass range of 0-100, the typical POM peaks (31, 61, 89) are more intense on the rough side (plasma treated). The smooth area (untreated) shows more signs of Na and Si. In the mass range of 100-300, peaks are more intense at mass 147, 221 and 281 on the smooth side (untreated). These peaks are typical of silicone (PDMS). The plasma process also has a cleaning effect.

Adhesion tests

It is often assumed that the functional groups on the surface contribute most to the quality of the adhesion between substrate and glue. Some of the most important ones are the hydroxyl group (-OH), the amino group (-NH₂) and the carboxyl acid group (-COOH). Atmospheric plasma treatment makes it possible to deliberately integrate these functional groups into the surface (Liebermann & Lichtenberg, 2005).



Picture 8 It is evident that bond strength is only significantly enhanced once the phase transition at the surface occurs (cohesive fracture patterns are observed). The area where only the surface energy is maximized only shows marginally improved bond strength.

Discussion

The effect of plasma treatment onto a surface is of a thermal, chemical and electrical nature and depends on the process parameter settings. Working distance, type of process gas, excitation power and processing speed play a crucial role, as well as the substrate characteristics. The thermal effects have already been analyzed in detail in a separate article (Nettesheim, Korzec, & Burger, 2015). In the following, the qualitative benefits of plasma surface treatment for adhesive bond strength are discussed exemplified by POM.

The effect most often cited, and maybe also the most obvious one, is that the surface is cleaned of contaminations which, as loosely bound separating layers, may dramatically weaken the adhesive bond (Kanegsberg & Kanegsberg, 2011). These contaminations may either be transferred onto the plastic surface during the production process, e. g. when separating agents are applied in mold building or injection molding, or afterwards during storage or handling. Segregation of low-molecular components from the plastic volume to the surface have also been reported. In the case under discussion, traces of sodium and PDMS are detected. However, as even samples carefully cleaned with solvents do not exhibit any dramatic changes in surface energy, the negative impact of residual contamination on the quality of the bonding seems negligible.

The atomic force microscopy images do not confirm any substantial macroscopic roughening of the surface which might be suspected due to the shift from shiny to matt. In a technical sense, the surface

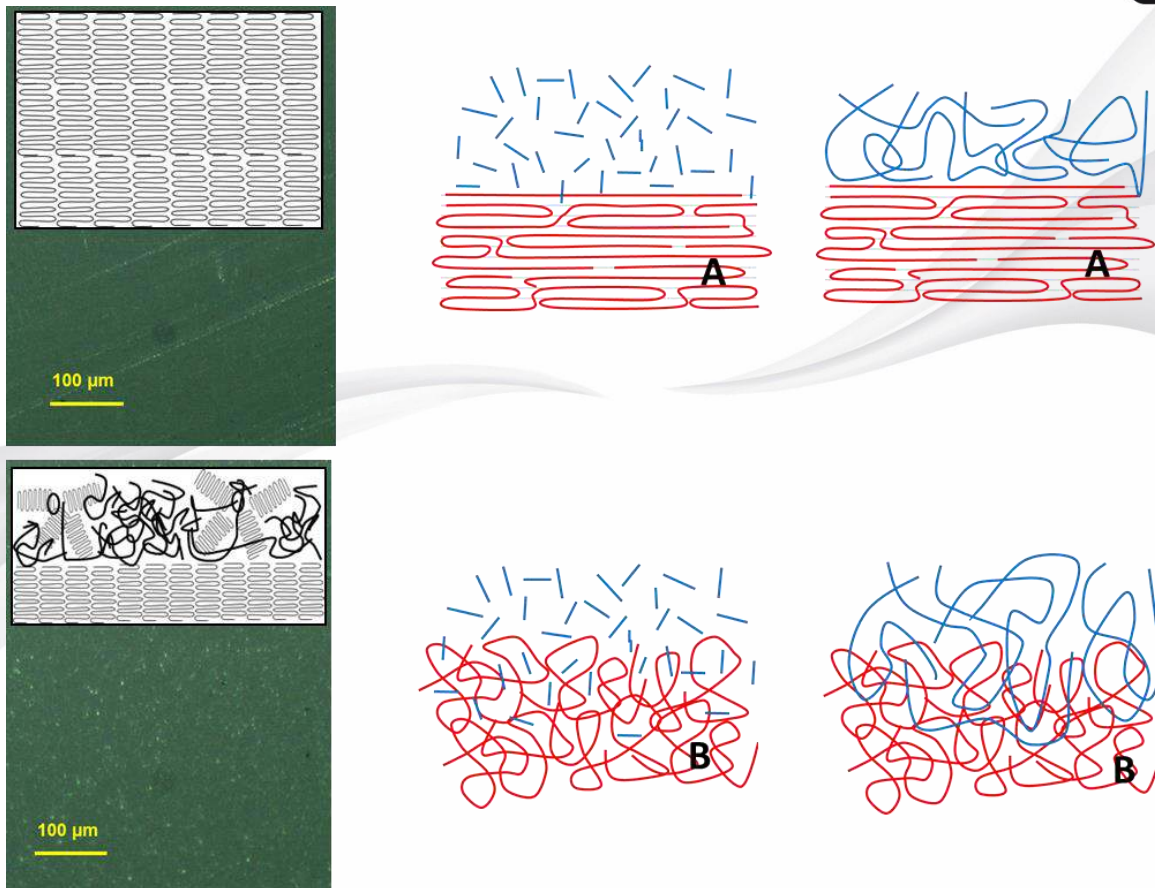
remains smooth, and the optical impression changes due to the altered diffuse light scattering in the layer close to the surface.

The fundamental contribution of functional chemical surface groups to the bonding of different polymer materials is well documented (Firas Awajaa, 2009). However, the quantitative contribution to the technically relevant quality of the bonding is often discussed controversially. The case of POM shows that atmospheric plasma treatment only alters the surface energy relatively slightly and the change effected is independent of the process gas used (nitrogen or air). Further, it can be observed that the choice of treatment intensity which is suited to maximize surface energy does not produce ideal combinations for tensile shear tests. Mass spectroscopy images show a minor change in oxygen concentration at the surface of the samples. Nitrogen is not found in any relevant concentrations.

The temperature of the surface and the layer close to it is dynamically increased during atmospheric plasma treatment if typical output density and traversing speed settings are chosen. Once a certain threshold is crossed, the phase transition temperature of the polymer is exceeded in this layer. However, both the heating and the cooling phase are limited to a thin layer and a short time span. Thus, this dynamic temperature effect determines the melting and crystallization behavior of the polymer material. In contrast to a thermoplastic polymer slowly solidified from cooling the molten bulk, new phase mixtures are formed near the surface in this process.

In addition to spherulitic superstructures, dendritic superstructures are also known (Ehrenstein, 2011). They form when there is a distinct temperature gradient inside the sample. The crystallization begins in the colder area, preferentially at imperfections, and the crystalline areas grow in the direction of areas with higher temperatures. In order to improve the quality of the mechanical material properties and to facilitate processing, various additives are employed: nucleating agents, demoulding aids, and modifiers to enhance scratch resistance (Kresta, 2013).

The turbidity observed in the sample surface points to a mixed phase of amorphous and crystalline areas which have been frozen due to the fast cooling process and therefore coexist in one thin layer. This causes differences in the refractive index and light diffusion (Bower, 2008). Literature states that the diffusion of components with low molecular weight is significantly higher in the amorphous phase than in the crystalline phase (Dröscher, 1976) (Menges, Haberstroh, & Michaeli, 2002). When a glue which hardens through polyaddition is applied to an amorphous polymer structure, the monomers can diffuse very well into the open structures of the amorphous polymer before the curing process is completed. The improved adhesion achieved with reactive glues can be interpreted in this model as an optimized interlinking of the glue's polymer chains with the polymer chains of the substrate (see picture 8).



Picture 9 Interpretation of the adhesion model.

Summary

Through a combination of various methods, the example of the thermoplastic polymer POM was used to show that in the course of surface treatment with a pulsed atmospheric plasma generator, a thermally induced phase transition from crystalline to amorphous can be observed. This transition is crucial for improving the joining properties with reactive 2K adhesive systems

Binnig, G., Quate, C. F., & Gerber, C. (1986). Atomic Force Microscope. *Physical Review Letters*, S. 930–933.

Bonhoeffer, K. (1924). *Zeitschrift der physikalischen Chemie*, 113, S. 199.

Bower, D. I. (2008). *An Introduction to Polymer Physics*. Cambridge University Press.

Dröscher, M. (1976). Ordnungszustände in Polymeren. *Chemie in unserer Zeit*, S. 106–113.

Ehrenstein, G. W. (2011). *Polymer-Werkstoffe: Struktur- Eigenschaften- Anwendung*. Carl Hanser Verlag GmbH & Co. KG.

Firas Awajaa, *. M. (2009). Adhesion of polymers. *Progress in Polymer Science*, S. 948-968.

Fridman, A. (2012). *Plasma Chemistry*. Cambridge: Cambridge University Press.

Hemsley, D. (1989). *Applied polymer light microscopy*. London: Elsevier Applied Science.

Kaelble, D. H. (1970). Dispersion-Polar Surface Tension Properties of Organic Solids. *Journal of Adhesion*, S. 66-81.

Kanegsberg, B., & Kanegsberg, E. (2011). *Handbook for Critical Cleaning: Applications, Processes, and Controls*. Taylor & Francis Inc.

Kresta, J. E. (2013). *Polymer Additives (Polymer Science and Technology Series)*. Springer.

Liebermann, M. A., & Lichtenberg, A. (2005). *Principles of Discharges and Materials Processing*. New Jersey: Wiley.

Menges, G., Haberstroh, E., & Michaeli, W. (2002). *Plastics Materials Science*. München: Hanser.

Nettesheim, S., Korzec, D., & Burger, D. (2015). Plasmaaktivierung von Rolle zu Rolle. *Adhäsion*, 20-25.

Owens, D., & Wendt, R. (1969). Estimation of the Surface Free Energy of Polymers. *J. Appl. Polym. Sci.*, S. 1741-1747.

R. Seliger, J. W. (1979). A high-intensity scanning ion probe with submicrometer spot size. *Appl. Phys. Lett.* 34 (5), S. 310.